EJSIT
European Journal of Science, Innovation and Technology
ISSN: 2786-4936
www.ejsit-journal.com
Volume 3 | Number 6 | 2023

Performance Monitoring of a Multi-Phase Desander with a Flow Control System

Tamunobere, A. A.*, Sodiki, J. I., Lebele-Alawa, B. T., Nkoi, B.
Department of Mechanical Engineering,
Rivers State University, Port Harcourt, Nigeria

ABSTRACT

Effective performance of multiphase desanders is crucial and of high importance to oil and gas field operator. Systems have been designed to ensure that the operation of desanders are carried out with close monitoring of the fluid stream and proper determination of the mechanical properties. The flow profile and other variables must be properly studied for effective separation of solids, these include the temperature, pressure, and flow rate of the feed fluid. The steady state of these parameters is crucial to the functionality of the desander hence controlling the operating values with process control system is considered viable. This paper focused on application of control model and simulation of flow control process using proportional integral derivative controller to monitor and improve performance of multiphase desander. A simulation was carried out via Simulink embedded in MATLAB with flow rate set at $0.055m^3/s$ as the operating parameter. The flow control mechanism used was venturi meter and simulation on manual and automatic mode operation carried out. From the simulation result obtained the controller attained stability in 66.7 seconds with PID values of 1.9235, 0.17402/s and -0.68991s respectively for automatic mode operation and 46.7 seconds with PID values of 10, 16/s and 14s respectively in manual operation mode. It is recommended to install multiphase desander with flow control process to enhance effective processing of crude oil stream.

Keywords: Hydrocyclone, Multi-phase desander, Separation efficiency, Flow control process

INTRODUCTION

One critical activity for operators in the oil and gas industry is the processing of reservoir fluid from oil wells. Most of these reservoirs have unconsolidated formations hence crude oil produced are entrained with solid particles that pose serious threat to sub-surface and surface equipment used in the processing of crude oil. The consequence amount to huge cost expended annually to repair damaged surface equipment including revenue loss owing to frequent shutdown of processing facilities. The installation of multiphase desander upstream of the processing equipment to effectively remove solid particles has contributed immensely to a reduction in the repairs of damaged equipment arising from erosion. Apart from being a useful tool for effective separation of solids, its functionality needs to be enhanced to improve performance while maintaining stability of the operating parameters by use of control process to give desired solid separation efficiency. In this study, attention is on incorporation of flow control process on the operation of the multiphase desander for effective solid-liquid separation of crude oil stream. Research done by same author and currently in press looked at the design and performance monitoring of a multiphase desander using a temperature control system. In that work a hydrocyclone (multiphase desander) was simulated and the separation efficiency was between 60 and 85% for solid particle sizes ranging from $3\mu m$ to $35\mu m$. whereas those with the range of 15 to $35\mu m$ achieved efficiency of 86 to 100%. In this study, a flow control process using Proportional Integral Derivative (PID) controller was applied to manage

* Corresponding Author

disturbances arising from flow abnormalities against planned value which on the overall constitute production off-set.

Rawlins (2018) published an article on the particle transfer between the cyclone and accumulator sections of a desander and emphasis was on the limiting fluid flux. The settling of solids from the cyclone to the accumulator follows turbulent and hindered-settling relationship that can be approximated by models used for sedimentation hoppers.

Rawlins (2002) worked on the application of multiphase desander technology to oil and gas production in which multiphase desander was designed and employed since 1995, for the separation of sand from well fluid. The background and application of multiphase desander was the focus of this paper. The models showing pressure drop and separation efficiency was done and logically presented based on literatures from Yoshioka and Hotta (1955); Bradley (1965); Rietema (1961); Holland-Batt (1980); Svarosky (1984) for the underflow desanders.

Azimian and Bart (2017) in a publication on numerical analysis of hydroabrasion looked at CFD model in developing the velocity profiles and separation efficiency curves of a hydrocyclone and how it can be predicted. The study employed the application of Euler-Euler model using computational fluid dynamics tool ANSYS-CFX 14.5.

Rawlins (2013) conducted further research on sand management methodologies for sustained facilities operations. Predicting the rate of natural solids production was a difficult challenge due to changing well conditions and getting data from the reservoir. Sand monitoring and measurement devices are available for detecting catastrophic sanding events or providing online measurement of sand concentration.

Huang et al. (2009) in their study on Application and operation optimization of hydrocyclone for solid-liquid separation in power plant looked at the use of hydrocyclone to separate solids from waste products released from power plant as pollutants. These are gypsum slurry and waste water. Others are ash, chloride ion and others that emirate from the operation of power plant. The publication looks at the theory and application of hydrocyclone in WFGD (Wet Flue Gas Desulfurization).

The objective of this study is to enhance the performance of multiphase desander with the incorporation of flow control process. With a flow control mechanism, the separation efficiency of hydrocyclone will be greatly improved owing to the elimination of disturbances arising from flow variation. This work was leveraged on the works carried out by Rawlings (2013). In the study the application of a multiphase desander in removing solids from crude oil fluid stream was highlighted making possible longer operation time including reduced shutdown of processing facilities and equipment maintenance which has been a major challenge in the oil and gas industry. The study provided a good understanding of how sand monitoring and measurement devices were deployed to detect sand production from wells that have catastrophic tendencies on surface processing equipment and in most cases downhole equipment. The study however suggested further work to improve the performance of multiphase desander in solid-liquid separation. This work therefore has provided related measures to improve multiphase desander performance with the incorporation of controls on the operating parameters such as inlet pressure, flow rate and temperature of feed fluid.

MATERIALS AND METHODS

Materials

Materials used for this study include thermodynamic data and software. Some of the materials include the use of collected operational data for simulation of the various models to validate the results obtained. The data were obtained from one of the multinational oil and gas companies operating in Nigeria.

Methods

Methods used for the study include fluid flow equations, hydrodynamics models, continuity equations, application of Newton's laws of forces, Laplace transform techniques, and material and energy balance principles.

Transfer functions derivative for flow control

The disturbances for the solid-liquid separation of crude in the desander (multiphase hydro cyclone) are flow rates, pressure P, temperature T, and level, h.

In this study the disturbances relating to flow rate were measured, checked with standard value (set point) and compared, to check the error signals back to the controller using a feed backward control loop. A mathematical model of the hydrocyclone was applied based on flow as disturbance variable and converted to transfer functions, a control environment of the process using Laplace Transform approach. The equation that describes the hydrocyclone behavior in terms of disturbance variables is based on the material and energy equations stated as

$$\left\{\begin{matrix}\text{Accumulation rate of materials}\\ \text{within the hydrocyclone}\end{matrix}\right\} = \left\{\begin{matrix}\text{Input rate of materials}\\ \text{into the Hydrocyclone}\end{matrix}\right\} - \left\{\begin{matrix}\text{Output rate of materials}\\ \text{from the Hydrocyclone}\end{matrix}\right\} \quad (1)$$

The material and energy block diagram showing the inflow, accumulation and outflow of disturbance variables is shown in Figure 1.

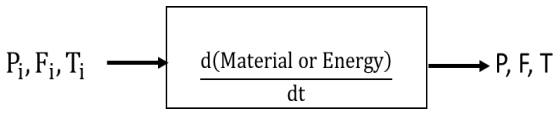

Figure 1: Schematic of Hydrocyclone Block Diagram Indicating Material and Energy Balance

From the block diagram in Figure 1 and applying equation (1), the mass balance equation is given as

$$\frac{d}{dt}(\rho V) = \rho_i, F_i - \rho_o F \quad (2)$$

where $\rho =$ Density of the fluid stream within the hydocyclone
$V =$ Volume of the fluid stream
$\rho_i =$ Density of the fluid stream entering the hydrocyclone
$F_i =$ Initial flow rates of the fluid

For constant density flow (incompressible fluid)

$$\rho = \rho_i = \rho_o \quad (3)$$

Also, in terms of level of the flow,

$$V = Ah \quad (4)$$

where $A =$ Area of the Hydrocyclone
$h =$ height/level of the flow

Combining Equations (2) and (3) into (1) gives

$$\frac{d}{dt}(\rho Ah) = \rho F_i - \rho F$$

$$\frac{Adh}{dt} = F_i' - F' \quad (5)$$

In terms of deviation variables, Equation (4) becomes

$$\frac{Adh'}{dt} = F_i' - F' \quad (6)$$

where $h' = h - h_s$
where h = deviation variable of the height,
h_s = steady state height.

$$F_i' = F_i - F_s$$

where F_i' is deviation variable of initial flow rate, F_i is steady state initial flow rate
F_s = steady state flow rate

$$F' = F - F_s$$

where F' = deviation volumetric flow rate. The transfer function of the hydrocyclone process that defined the control in terms of flow is given by the Laplace Transform of Equation (5) as

$$\mathcal{L}\left\{\frac{h'}{dt}\right\} = \frac{1}{A}\{\mathcal{L}\{F_i'\} - \mathcal{L}\{F'\}\}$$

$$s\bar{h}_{(s)} - h_{(o)} = \frac{1}{A}\left(\bar{F}'_{i(s)} - \bar{F}'_{(s)}\right) \quad (7)$$

Note that $h_{(o)} = o$, and let $a = \frac{1}{A}$. Then Equation (7) is written as

$$s\bar{h}_{(s)} = a\bar{F}'_{i(s)} - a\bar{F}'_{(s)} \quad (8)$$

The relationship between flow rate and level is given by

$$F \propto h^{1/2} \quad (9)$$

$$=> F = a'\sqrt{h} \quad (10)$$

where a' = constant related in terms of specific gravity, density, ρ, acceleration due to gravity, g, velocity of the flow, u and area of flow.

The term $h^{1/2}$ is a non-linear term hereby linearized using Taylor's series expansion as (Zill, 2017)

$$f(h) = f(h_o) + (h - h_o)f'(h_o) + \cdots \quad (11)$$

$$f'(h_o) = \left[\frac{1}{2}h^{\frac{1}{2}-1}\right]_{h_o} =$$

$$\frac{1}{2}ho^{-1/2} = \frac{1}{2\sqrt{h_o}} \quad (12)$$

where h_o = initial level

Applying Equations (10) and (11) into (10) gives

$$F = a'\left\{\sqrt{h_o} + (h - h_o)\left(\frac{1}{2h_o^{1/2}}\right)\right\} \quad (13)$$

$$F = a'\left\{\sqrt{h_o} + \frac{1}{2\sqrt{h_o}}h - \frac{1}{2}\sqrt{h_o}\right\}$$

$$F = a'\left\{\frac{1}{2}\sqrt{h_o} + \frac{1}{2\sqrt{h_o}}h\right\} \quad (14)$$

But $\mathcal{L}\{F'\} = a'\left\{\mathcal{L}\left\{\frac{1}{2\sqrt{h'_o}}\right\} + \frac{1}{2\sqrt{h_o}}\mathcal{L}\{h'\}\right\}$

$$\bar{F}'_{i(s)} = a'\left\{\frac{\sqrt{h'_o}}{2s} + a_1\bar{h}'_{(s)}\right\} \quad (15)$$

where h'_o = deviation variable for the height/level initially, h = deviation level/height

$$a_1 = \text{constant} = \frac{1}{2\sqrt{h_o}}$$

Substituting equation (14) into Equation (7) yields

$$s\bar{h}'_{(s)} = a\,\bar{F}'_{i(s)} - a\left(a'\frac{\sqrt{h'_o}}{2s} + a'a_1\bar{h}'_{(s)}\right) \quad (16)$$

Let $aa'a_1 = a_2$, and $aa' = a_3$, then Equation (16) becomes

$$s\bar{h}'_{(s)} = a\,\bar{F}'_{i(s)} - a_2\bar{h}'_{(s)} = \frac{a_3\sqrt{h'_o}}{2s}$$

$$(s + a_2)\bar{h'}_{(s)} = a\,\bar{F}'_{i(s)} - \frac{K}{s} \tag{17}$$

where $K = \frac{a_3\sqrt{h'_o}}{2}$

The transfer function for Equation (16) used for controlling level/height is given as

$$G_{P_{1(s)}} = \frac{\bar{h'}_{(s)}}{\bar{F}'_{i(s)}} = \frac{a}{s+a_2} \tag{18}$$

$$G_{d_{(s)}} = \frac{K}{s(s+a_2)} \tag{19}$$

where $G_{d_{(s)}}$ is the disturbance transfer function

The general transfer function response for the PID control system of the level hydrocyclone is stated as (Stephanopolous, 2008)

$$\bar{h'}_{(s)} = \frac{G_{P_{(s)}} G_{f_{(s)}} G_{c_{(s)}}}{1 + G_{P_{(s)}} G_{f_{(s)}} G_{c_{(s)}} G_{m_{(s)}}}\, h'_{sp(s)} + \frac{G_{d_{(s)}}}{1 + G_{P_{(s)}} G_{f_{(s)}} G_{c_{(s)}} G_{m_{(s)}}}\, h'_{d(s)} \tag{20}$$

where $G_{f_{(s)}}$ is the transfer function of the (valve),

$G_{C_{(s)}}$ = transfer function of the PID controller

$G_{m_{(s)}}$ = transfer function of the measured variable.

This $G_{c_{(s)}}$ is stated generally as

$$G_{c_{(s)}} = \frac{C_{(s)}}{\varepsilon_{(s)}} = k_c\left\{1 + \frac{1}{\tau_I s} + \tau_D s\right\} \tag{21}$$

where k_c is the PID gain, τ_I is the integral constant and τ_D is a derivative constant.

Here, a venturi meter is the measuring device for the control of flow rate.

Noting that $G_{f_{(s)}} = G_{m_{(s)}} = 1$, then Equation (20) is transformed as

$$\bar{h'}_{(s)} = \frac{\left(\frac{a}{s+a_2}\right)k_c\left\{1+\frac{1}{\tau_I s}+\tau_D s\right\}}{1+\left(\frac{a}{s+a_2}\right)k_c\left\{1+\frac{1}{\tau_I s}+\tau_D s\right\}}\, h'_{sp(s)} + \frac{\frac{k}{s(s+a_2)}}{1+\left(\frac{a}{s+a_2}\right)k_c\left\{1+\frac{1}{\tau_I s}+\tau_D s\right\}}\, h'_{d(s)} \tag{22}$$

RESULTS AND DISCUSSION

Figure 2 shows the configuration of the control process using a flow meter to measure the flow rate for comparing with the set point. The simulation was carried out in SIMULINK MAT-LAB. The block diagram is a closed loop feedback PID flow controller and shows the transfer function and the necessary step input for smooth process response. Figure 3 shows the result of manual tuning of the process, with chosen PID 10, 16/s, 14s values to stabilize the process, with a view to achieve the required response. This resulted in nearly stabilized response after the initial overshoot. The process, therefore, needed further tuning. Figure 3 shows the result of further tuning of the process with a different set of PID values 15,10/s,7s with a view to achieve the required response. This again resulted in an unstable output given the existence of overshoot. Therefore, the desired result was not achieved and the controller required further tuning. Figure 4 shows the amplitude of response robustness of the controller to achieve the desired response. PID values were selected accurately by the controller to achieve stability. Table 1 shows the corresponding input data for the controller with flow rate as the operating parameter. The tuned values were those automatically selected by the controller as compared to the block values that were manually chosen to attain stability.

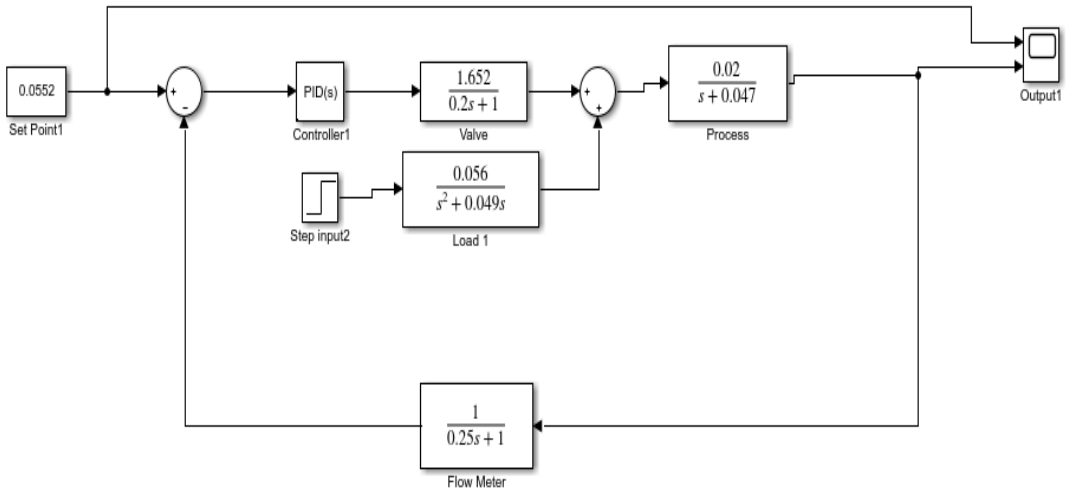

Figure 2: Block Diagram for a Closed Loop Feedback for PID Control System of Flow Rate

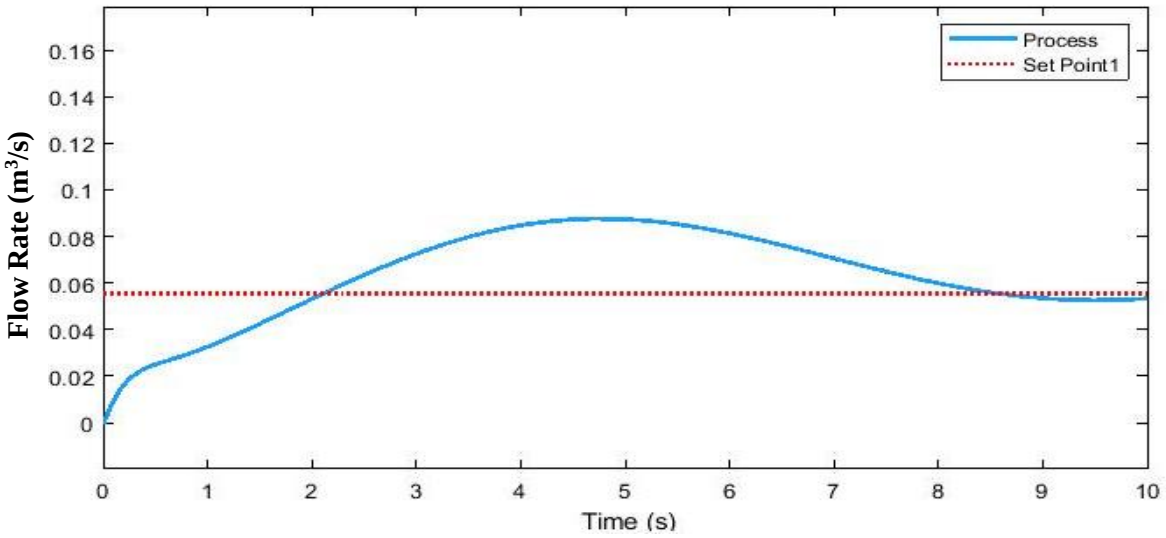

Figure 3: Flow Rate vs Time Graph of the Controller with PID Values of 10,16/s,14s

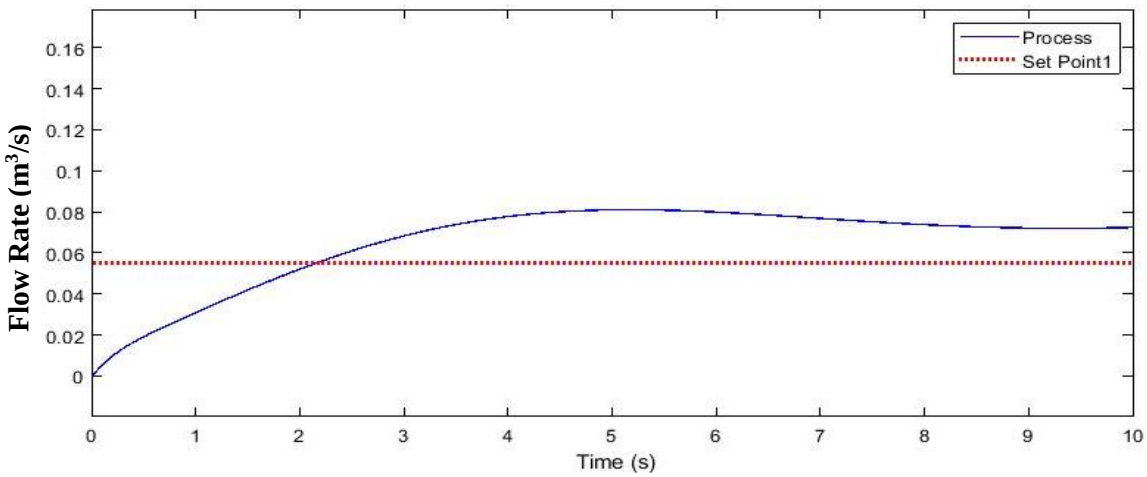

Figure 4: Transient Response Amplitude vs Time Graph of Flow Rate Controller with Tuned and Blocked Values

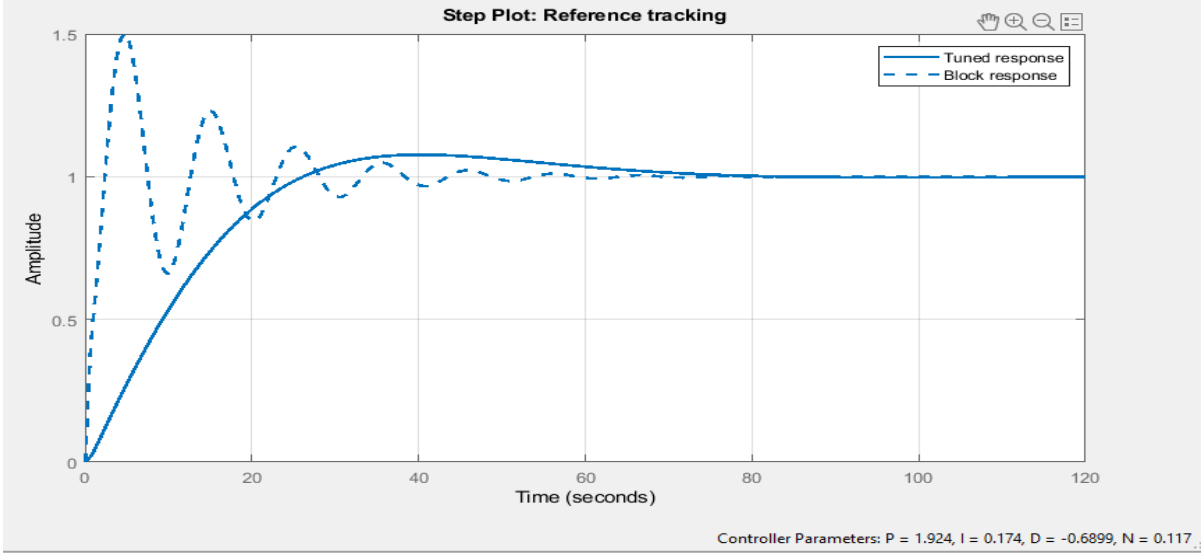

Figure 5: Flow Rate vs Time Graph of the Controller with PID Values of 15,10/s,7s

The performance could be compared between the tuned and block values. The result further shows the corresponding input data for the controller robustness in processing the input to achieve the desired response with flow as the control variable. The tuned curve was for data generated by the system whereas the block curve was for data selected manually to monitor the PID controller performance.

As regards the overall performance of the controller, the rise time for the selected data showed that it was achieved in 1.89 seconds giving a sudden rise in value above the set point with a huge overshoot. The process shows that it took 66.7 seconds to settle before completing stability for the tuned values. On the contrary, the process took 46.7 seconds to complete stability for the manually selected PID values. Both sets of data gave a stable control process but the performance was different.

Table 1: Controller Parameters for Automatic and Manual Flow Rate Control

Controller Parameters	**Tuned**	**Blocked**
P	1.9235	10
I	0.17402	16
D	-0.68991	14
N	0.11704	100
Performance and Robustness	**Tuned**	**Blocked**
Rise time	18.5 seconds	1.89 seconds
Settling time	66.7 seconds	46.7 seconds
Overshoot	7.7%	49.9%
Peak	1.08	1.5
Gain margin	43.2 dB @ 4.42 rad/s	39.8dB @ 29.1 rad/s
Phase margin	69 deg @ 0.0823 rad/s	19.3 deg @ 0.628 rad/s
Closed-loop stability	Stable	Stable

Furthermore, the manually tuned process response was fast to correct the overshoot when compared with the automatic mode of operation. The rise time for the automatically manipulated process was higher but the overshoot was very small.

The manipulated PID values (9,4/s,10s) to operate the controller initially showed a huge overshoot of 0.5mm and stabilized to the set point after 60 seconds.

The rise time was 18.5s for the automatic mode whereas the manual mode resulted in 1.89s; and settling time was 66.7s and 49.9s respectively. This shows that it took less time for the process to reach the desired output with manually selected PID data.

CONCLUSION

Considering flow rate as the operating parameter, the result shows that the PID process controller overall settling time before completing stability was 58.8 seconds for the tuned operating mode, whereas the manually manipulated operating mode recorded 9.84 seconds to complete stability. It took more time for the controller to attain stability in the automatic operating mode compared to the manual mode.

NOMENCLATURE

English Symbols

F Flow Rate [m^3/s]
h Level [m]
P Pressure [N/m^2]
T Temperature [K]
t Time [s]

Greek Symbols

ρ Fluid Density [kg/m^3]

REFERENCES

Azimian, M. & Bart, H. J. (2017). Numerical Analysis of Hydroabrasion in a Hydrocyclone. *Petroleum Science, 13,* 304-319.

Holland-Batt, A. B. (1980). A Bulk Model for Separation in Hydrocyclones (Paper Presentation). *3rd International Conference on Multiphase Technology in Banff,* Alberta, *9*(1), 2-14.

Huang, I., An, L-S., Wu, Z-Q. (2009). Study of Application and Operation Optimization of Hydrocyclone for Solid-Liquid Separation in Power Plant. *Proceedings of the World Congress on Engineering and Computer Science,* I, 20-22. San Francisco.

Rawlins, C. H. (2002). Application of Multiphase Desander Technology to Oil and Gas Production. Kvaerner Process Systems US. *Presented at the 3rd International Conference on Multiphase Technology* in Banff, Alberta, 3-5 June.

Rawlins, C. H. (2013). Design of a Cyclonic Solids Jetting Device and Slurry Transport System for Production Systems. *Paper 166118 presented at the SPE Annual Technical Conference and Exhibition,* New Orleans, Louisiana, 30 Sep-02 Oct.

Rawlins, C. H. (2018). Particles – Transfer between the Cyclone and Accumulator Sections of a Desander. *Society of Petroleum Engineers, (SPE 191147) Production & Operations,* 1-10.

Rietema, K. (1961). Performance and Design of Hydrocyclones I–General Considerations. *Chemical Engineering Science, 15*(1), 298-302.

Stephanopoulos, G. (2008). *Chemical Process Control: An Introduction to Theory and Practice*. Prentice-Hall, Englewood Cliffs, New Jersey 07632.

Svarovsky, L. (1984). *Hydrocyclones*. Lancsater, P A: Tecnomic Publishing Co., Inc.

Yoshioka, N. & Hotta, Y. (1955). Liquid Cyclone as a Hydraulic Classifier. *Kagaku Kogaku Ronbunshu, 19*(1), 632-641.

Zill, D.G. (2017). *Advanced Engineering Mathematics* (6th ed.). Massachusetts: Jones & Bartlett Learning.